



# Microstructure Characteristics and Mechanical Properties of Al-12Si Coatings on AZ31 Magnesium Alloy Produced by Cold Spray Technique

Yi Hao, Ji-qiang Wang, Xin-yu Cui, Jie Wu, Tie-fan Li, and Tian-ying Xiong

(Submitted August 20, 2015; in revised form March 20, 2016)

The cold spray technique was used to deposit Al-12Si coatings on AZ31 magnesium alloy. The influence of gas pressure and gas temperature on the microstructure of coatings was investigated so as to optimize the process parameters. OM, SEM, and XRD were used to characterize the as-sprayed coatings. Mechanical properties including Vickers microhardness and adhesion strength were measured in order to evaluate coating quality. Test results indicate that the Al-12Si coatings possess the same crystal structure with powders, sufficient thickness, low porosity, high hardness, and excellent adhesion strength under optimal cold spray process parameters.

**Keywords** Al-12Si coatings, cold spray, mechanical properties, microstructure, porosity

## 1. Introduction

As a lightweight material for industry application, magnesium and its alloys possess attractive physical and mechanical properties, such as low density, high specific strength and stiffness, high thermal conductivity, and excellent machinability (Ref 1, 2). These outstanding properties make them increasingly applied in the automotive, aerospace, electronics, and transportation industries (Ref 3, 4). Nonetheless, the main impediments against wider applications are undesirable properties including poor plasticity, heat resistance, abrasion resistance, and corrosion resistance. In particular, the abrasion and corrosion are two of the most commonly encountered industrial problems generating the frequent replacement of some engineering components and an increase in total costs (Ref 5). These problems must be solved before the alloys are used in a wider scope of applications.

The use of coatings is one of the most effective methods to protect magnesium and its alloys against rapid failure in harsh conditions. At present, various surface techniques are utilized to prolong the service life of magnesium and its alloys. These include cold spray (CGDS) (Ref 1, 4), thermal spray (Ref 6), electroplating (Ref 7), electroless plating (Ref 8), physical vapor deposition (Ref 9),

laser/electron beam surface modification (Ref 10, 11), ion implantation (Ref 12), microarc oxidation (Ref 13), chemical conversion treatment (Ref 14, 15), etc. It is well known that magnesium and its alloys possess such high chemical activity and poor abrasion resistance that a majority of surface techniques cannot provide long-time protection in diverse and complex service environments. Cold spray is a low-temperature deposition process, which produces much harder, thicker, and denser coatings.

During the cold spray process, powder particles are accelerated to high velocity in a supersonic gas jet produced via a converging-diverging De Laval nozzle. When these powder particles impinge on the substrate, a coating is formed by severe plastic deformation. Cold spray provides a promising alternative to produce a broad range of metallic, non-metallic (e.g., ceramic, organic polymer), composite, and novel coatings (e.g., nano, amorphous) (Ref 16–24) due to its unique characteristics of high density, low oxidation, low residual stress, and high deposition efficiency at low temperature. Hence, cold spray possesses a great potential for applying coatings in military, steel, aerospace, energy, and chemical engineering fields.

Two main types of protective coatings are wear-resistant coatings and corrosion-resistant coatings. Al coatings are an example of providing protection (Ref 4, 16, 25–27). The Al-Si alloys have excellent wear resistance which is one of the main reasons for wide applications in the automotive and aerospace industries. Clarke et al. (Ref 28) reported that the wear rate of an as-cast binary Al-Si alloy decreased with an increase in Si content and was the lowest for the eutectic composition. Previous research (Ref 29) showed the corrosion resistance of Al-Si alloys was much higher than Al in the atmosphere, fresh water, and organic acids. Thus, Al-Si alloys are considered to be a good choice for cold spray deposition. Baik et al. (Ref 30) observed that the wearable Al-Si alloy and its

Yi Hao, Ji-qiang Wang, Xin-yu Cui, Jie Wu, Tie-fan Li, and Tian-ying Xiong, Institute of Metal Research, Chinese Academy of Sciences, Shenyang 110016, People's Republic of China. Contact e-mail: tyxiong@imr.ac.cn.

composite coatings deposited via plasma spray were one of the important applications for clearance control of turbine engines. However, very few reports are available to help us understand Al-Si alloys or their composites by cold spray except some researcher's pioneering work (Ref 31-33). In our research, the first step was to optimize the preparation technology of cold-sprayed Al-12Si coatings on AZ31 magnesium alloy by observing the microstructure characteristics of Al-12Si coatings deposited at different process parameters. Then, the mechanical properties, including coating microhardness and abrasion strength between coating and substrate, were examined. Wear and corrosion behaviors of the coatings will be investigated in future work.

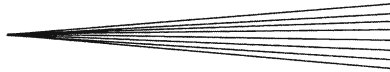
## 2. Experimental Procedures

### 2.1 Materials

The commercial available Al-12Si alloy powders were produced by gas atomization, and the chemical composition is presented in Table 1. The particle size distribution (PSD) of the powders was measured using a laser particle size analyzer (MS2000, Malvern, UK). The surface shape and cross-section characteristic of Al-12Si powder particles were observed using a scanning electron microscopy (SSX-550, Shimadzu, Japan) and an optical microscope (Axio Observer Z1M, Zeiss, Germany). The bulk substrate material investigated in this study was an as-cast AZ31 magnesium alloy, and its chemical composition is listed in Table 2. Prior to cold spray deposition, the substrate (12 × 10 × 2 mm) was ground by fine abrasive paper in order to remove linear-cutting traces, cleaned with alcohol, and then sandblasted using SiO<sub>2</sub> grit. The Al-12Si powders had to dry in vacuum drier at 60 to 70 °C for over 5 h before each use.

### 2.2 Cold Spray Process

The Al-12Si powders were deposited on the AZ31 substrate using cold spray equipment created by our research group. This equipment consisted of a standard De Laval (convergent-divergent) nozzle possessing the rect-



angular cross-section exit with an aperture of 2 × 10 mm and a rectangular throat of 2 × 3 mm. The system used compressed air as the accelerating gas and the carrier gas for powder feeding. The pressure of carrier gas should exceed that of accelerating gas to ensure powder transportation into the main flow. During the deposition process, the gas pressure was fixed at 1.4 and 1.8 MPa. The gas temperature ranged from 200 to 400 °C. The standoff distance from nozzle exit to substrate surface was maintained at 10 mm. Each spray pass was completed within 30 s. The substrate was fixed by a holder, and a spray gun moved at a constant speed of 100 cm/min above the substrate. The deposition process was controlled by pre-set program to ensure uniformity of Al-12Si coatings.

### 2.3 Coating Characterization Techniques

The microstructure characteristics of surface and cross section for the as-sprayed Al-12Si coatings were investigated by SEM. The coating porosity was measured using the metallographic image analysis software (SISC IAS V8.0) (Ref 1). Ten SEM micrographs at magnification of ×1000 were randomly captured for this measurement. Before SEM analysis of cross section, the specimens were cold mounted in denture acrylic to maintain the coating structure, and sequentially ground using increasingly finer SiC sandpapers and then polished with diamond pastes using alcohol to produce a surface without oxidation and scratches.

The phase identification of Al-12Si powders and the as-sprayed coatings was determined using an x-ray diffraction (D/Max-2500PC, Rigaku, Japan). The XRD analysis was carried out using a Philips X'Pert MPD diffractometer equipped with a graphite monochromator using Cu K $\alpha$  ( $\lambda = 0.15406$  nm) radiation. The diffraction pattern was recorded in the range of 10° to 90° 2 $\theta$  with 0.02° step width and 2 s per step acquisition time.

### 2.4 Mechanical Property Testing

The Vickers microhardness tests were performed on the coated specimens, AZ31 substrate, and Al-12Si powders using a microhardness tester (AMH43, Leco, USA) with 10, 50 g (HV<sub>10</sub>, HV<sub>50</sub>) loads and a dwell time of 15 s. Prior to microhardness test, all specimens were ground

**Table 1** The chemical composition of Al-12Si alloy powders used in this study

	Chemical composition, wt.%				
	Si	Fe	Zn	O	Al
Original Al-12Si powder	11.78	0.13	0.05	0.11	Bal.

**Table 2** The chemical composition of the as-cast AZ31 magnesium alloy used as the substrate for cold spray

	Chemical composition, wt.%								
	Al	Zn	Mn	Si	Cu	Fe	Ni	Ca	Mg
As-cast AZ31Mg alloy	3.03	1.01	0.32	<0.01	<0.005	<0.005	<0.005	<0.002	Bal.

and then polished to obtain the same roughness. The distance between two indentations was three times larger than that of diagonal in order to eliminate the effect of stress field from nearby indentations. The hardness values were the average of seven indentations for each specimen.

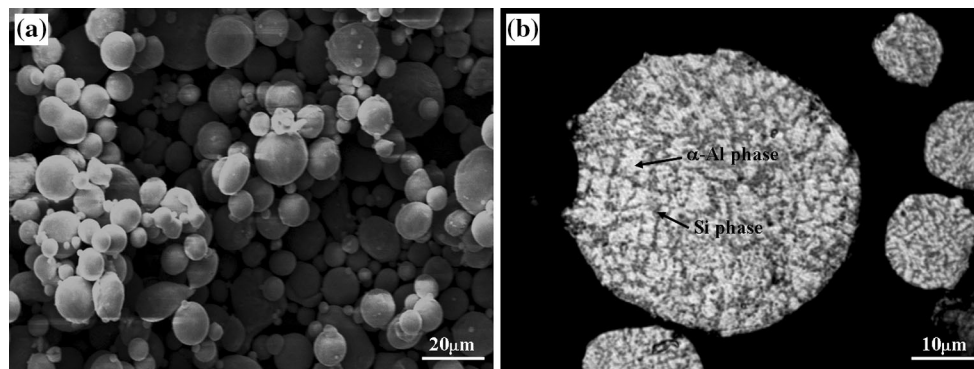
The adhesion strength between coating and substrate is an important mechanical performance index, which is used as a measure of coating quality. In this study, the adhesion of the as-sprayed Al-12Si coatings on AZ31 substrate was measured using an electronic tensile testing machine (AG-100KNG, Shimadzu, Japan). Prior to testing, the double-sides of the AZ31 specimens with a diameter of 25 mm and a length of 5 mm were grit blasted to obtain the desired surface roughness. After the coating was deposited on one side of each specimen, the specimen was bonded to a homemade cast-steel tensile fixture using E7 glue. The bond strength of E7 glue for Al and Mg materials can be as high as 70 to 80 MPa. The bonded samples were placed in an oven and cured at 105 °C for 3 h. The tensile testing was performed at room temperature (26 to 29 °C), and the strain rate was controlled at 1 mm/min. The adhesion strength values were the average of three measurements for each specimen.

### 3. Results and Discussion

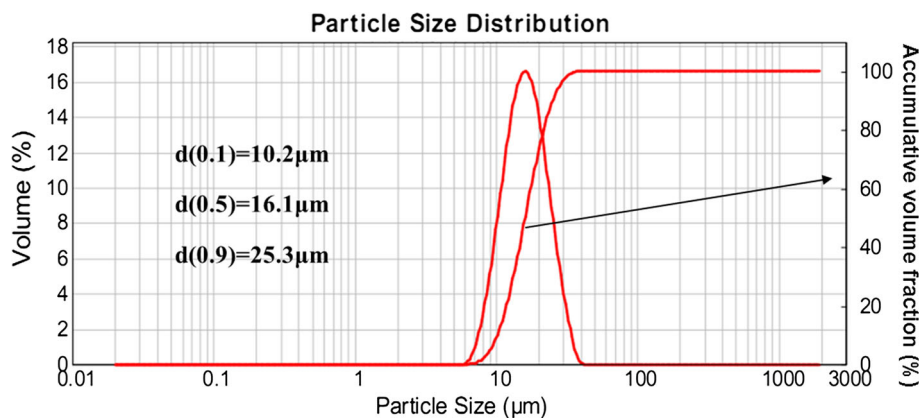
#### 3.1 Characteristics and Distribution of Al-12Si Powders

Figure 1 shows the morphology of Al-12Si powders and the cross section of several particles. The Al-12Si powders are sieved to 400 mesh ( $\leq 38 \mu\text{m}$ ) and exhibit a near-spherical shape, as shown in Fig. 1(a). From the cross section of particles shown in Fig. 1(b), a fine-scaled dendritic microstructure in which Si phase is formed between primary  $\alpha$ -Al dendrite arms can be observed. The composition of Al-12Si powders is quite close to the eutectic composition of 12.6%Si found in Al-Si binary phase diagram. The powder particles present the eutectic structure resulting from the eutectic reaction. OM result indicates the light areas in Fig. 1(b) are the aluminum-rich phase, and the darker areas are the silicon-rich phase.

Figure 2 illustrates the size distribution of Al-12Si powder particles. The size distribution of powders is  $d(0.1)$  of 10.2  $\mu\text{m}$ ,  $d(0.5)$  of 16.1  $\mu\text{m}$ , and  $d(0.9)$  of 25.3  $\mu\text{m}$ . As can be seen from volume fraction of particles, no Al-12Si powders are  $<6 \mu\text{m}$  in size, and the main size distribution of the powder particles is 10 to 30  $\mu\text{m}$ . So the diameters of



**Fig. 1** Morphology of Al-12Si powders (SEM micrograph, a) and cross section of several particles (Metallograph, b)



**Fig. 2** Size distribution of Al-12Si powder particles (volume fraction)

the spherical particles range from 6 to 40  $\mu\text{m}$ . However, there may be small measurement error because some larger particles (diameter  $> 40 \mu\text{m}$ ) might not have been counted due to the limitation of sampling during laser size measurement.

### 3.2 Influence of Gas Pressure on Al-12Si Coatings

Zhao et al. (Ref 31) found that Al-12Si coatings could not be produced by cold spray at the relatively low process gas temperature of 200  $^{\circ}\text{C}$  no matter how the other parameters were varied. Based on the above literature, 200  $^{\circ}\text{C}$  is used as the gas temperature in the first spray test. In addition, the gas pressure is set at 1.4 MPa which is a lower value compared with the values reported in the literature (Ref 32, 33). The experimental results demonstrate that an extremely thin Al-12Si coating is formed on AZ31 magnesium alloy using cold spray. However, when gas temperature is reduced to 150  $^{\circ}\text{C}$ , no Al-12Si is deposited on AZ31 substrate. It is concluded that the homemade cold spray equipment is able to produce Al-12Si coatings at relatively low gas pressure (1.4 MPa) and gas temperature (200  $^{\circ}\text{C}$ ). In this section, we mainly investigate the influence of gas pressure on thickness and quality of the coatings.

The gas pressure is fixed at 1.4 MPa, while the temperature ranges from 200 to 400  $^{\circ}\text{C}$ . Figure 3 provides surface SEM micrographs of a cold-sprayed Al-12Si coating deposited at 1.4 MPa and 200  $^{\circ}\text{C}$ . It is found that

the surface of the thin coatings is relatively flat, but a deep hole exists in a local region as shown in Fig. 3(a). As observed from Fig. 3(b), the formation of coating is attributed to a successive deposition of some deformed particles through continuous impact. The inner region of white box in Fig. 3(b) is magnified in Fig. 3(c), and it can be clearly seen that the deformed particles are in the size range from 6 to 11  $\mu\text{m}$ . In fact, the sizes of powder particles are even smaller than those of deformed particles as shown in Fig. 3(c). The phenomenon indicates that smaller particles preferentially reach critical velocities for deposition at the low process conditions of 1.4 MPa, 200  $^{\circ}\text{C}$ , while larger particles are bounced off when they impact on the substrate or the deposited coatings. Although the resilient larger particles have a strong punning effect on the deposited material, which helps generate the compact coatings, the thickness and quality of coatings fail to satisfy the demand due to low deposition efficiency. Figure 4 illustrates the cross-section morphology of Al-12Si coatings deposited at 1.4 MPa as a function of gas temperature. Comparing Fig. 4(a) to (c), the thickness of coating increases with the increase of gas temperature. It can be seen that the thickness of coating deposited at 400  $^{\circ}\text{C}$  is about ten times that of the coating deposited at 200  $^{\circ}\text{C}$ . However, the thicker coatings have an uneven thickness. Table 3 presents the variation in the thickness of three Al-12Si coatings deposited at 1.4 MPa. Taking the coating deposited at 300  $^{\circ}\text{C}$  as an example, it is found that the thickest region of coating is 70  $\mu\text{m}$ , and the thinnest region

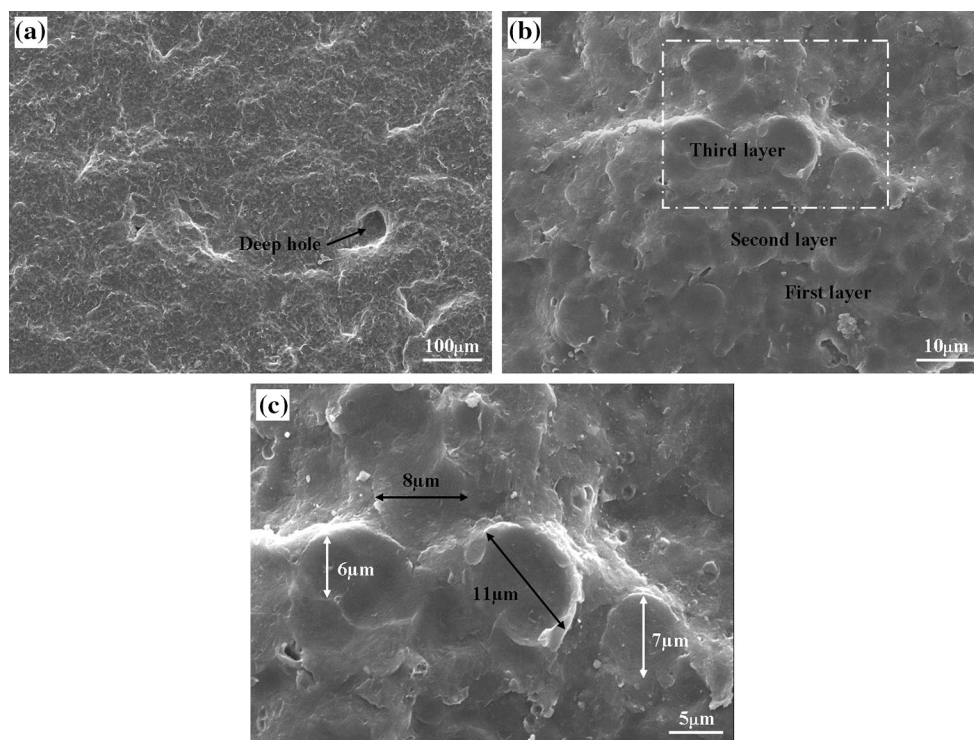


**Fig. 3** Surface SEM micrographs of a cold-sprayed Al-12Si coating deposited at 1.4 MPa and 200  $^{\circ}\text{C}$  (a overview; b, c-high magnification)

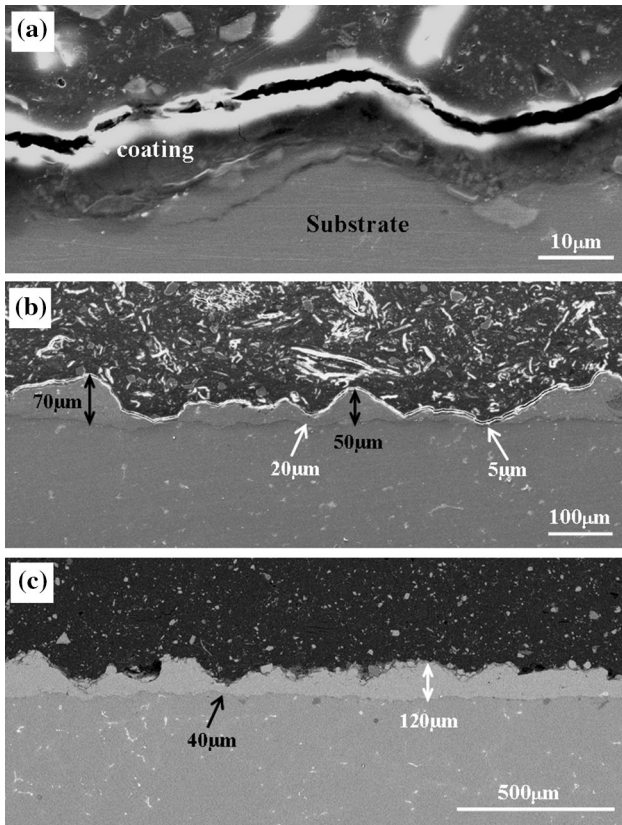


**Fig. 4** Cross-section morphology of Al-12Si coatings deposited at 1.4 MPa as a function of gas temperature (a 200 °C, SE; b 300 °C, SE; c 400 °C, BSE)

**Table 3** Variation in the thickness of three Al-12Si coatings deposited at a gas pressure of 1.4 MPa

Gas temperature, °C	200	300	400
Al-12Si coating thickness/ $\mu\text{m}$	3-12	5-70	40-120

is only 5  $\mu\text{m}$ . We draw a conclusion that an excellent Al-12Si coating could not be produced at a low gas pressure of 1.4 MPa even if gas temperature is increased to 400 °C. The gas pressure, therefore, is proven to be a critical factor during the cold spray process.

When the gas pressure is increased to 1.8 MPa and the gas temperature is set as 300 °C, the coatings have a coarser surface and more uniform thickness due to the deposition of larger particles than coatings deposited at 200 °C as displayed in Fig. 5 and 6, which shows the variations in surface morphology and thickness of Al-12Si coatings deposited at a gas pressure of 1.8 MPa and an increase in gas temperature. It can be seen that the influence of gas pressure on coatings at low gas temperatures is much smaller than that at high gas temperatures. Thus, the gas temperature also has a significant influence on coating quality and deposition efficiency.

### 3.3 Influence of Gas Temperature on Al-12Si Coatings

The particle velocity is a function of gas temperature. Under the same gas pressure, the appropriate increase of gas temperature is beneficial to increasing the speed of powder particles. Therefore, in this section, the main research is focused on the relationship between gas temperature and coating quality.

The SEM micrographs in Fig. 5 illustrate different surface features of Al-12Si coatings at 200, 250, 300, 350, and 400 °C, respectively. Comparing Fig. 5(a) to (e), it can be seen that the surface roughness of coatings increases with increasing gas temperature. The quantity of deformed particles in the coatings deposited at gas temperatures over 300 °C is larger than that in the coatings deposited at gas temperatures of 200 and 250 °C. Observed from enlarged view in Fig. 5(c), many larger deformed particles are found in the coatings, such as particles with sizes of 23 and 45  $\mu\text{m}$ . However, as shown in Fig. 5(e), the loose packing phenomenon between particles is observed at higher gas temperatures. The particles located on the top surface of coatings have little or no deformation due to the lack of peening effect of resilient particles. It is known that the enhanced gas temperature gives rise to a significant increase in coating thickness, and the variation in thickness is presented in Fig. 6. The different thicknesses of coatings are about 8, 15, 350, 600, and 2500  $\mu\text{m}$  in sequence when the gas temperature ranges from 200 to 400 °C at a gas pressure of 1.8 MPa. The cross-section micrograph of coatings deposited at 300 °C is shown in Fig. 6. The coatings deposited at 400 °C are more than 300 times thicker than those deposited at 200 °C. Such a great variation indicates the gas temperature plays a great role in increasing coating thickness. The increase in gas temperature increases the gas velocity and particle temperature which result in higher particle velocities. The higher velocities allow larger particles to reach critical deposition velocities. In addition to thickness, the porosity is also a vital factor for evaluating a cold-sprayed coating.

The micrographs in Fig. 7 indicate the influence of gas temperature on the porosity of Al-12Si coatings deposited at 1.8 MPa. It can be observed that the porosity of coatings deposited at a gas temperature of 300 °C is about 1.89%, while the porosities are about 4.80 and 11.71% for coatings deposited at gas temperatures of 350, 400 °C. The microstructures of these coatings deposited at 1.8 MPa and 300 to 400 °C are porosity, as shown in Fig. 8. The pores have a significant increase in size with increasing gas temperature because of interconnection between pores seen from cross section of coatings. In a word, the smaller porosity indicates the denser coating.

When the gas temperature is increased to 300 °C, the degree of deformation of the powder particles is greater than that of 200, 250 °C, resulting in a decrease of porosity. As a result, a much denser coating is produced by cold spray due to the impact effect of subsequent particles combined with the peening effect of resilient particles. However, an abnormal phenomenon occurs when the gas

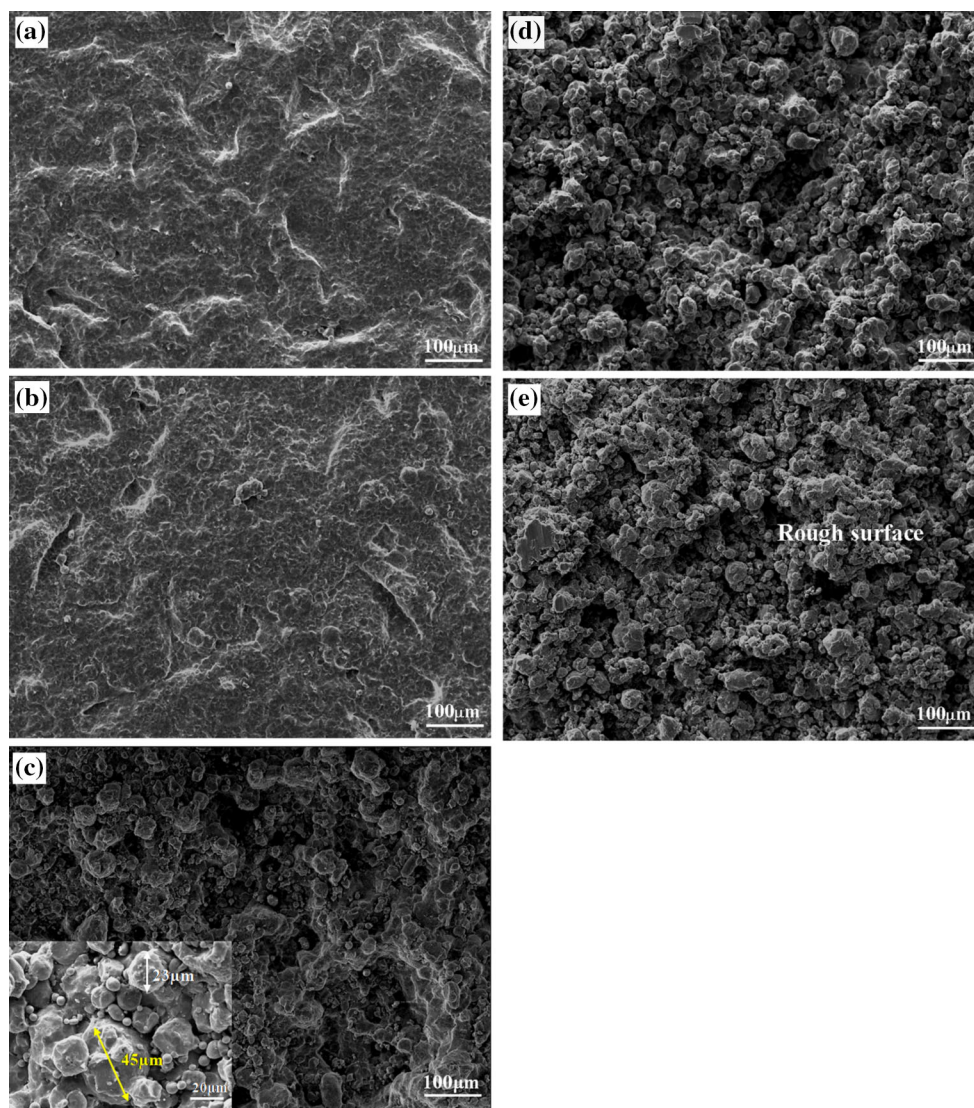


**Fig. 5** Surface morphology of Al-12Si coatings deposited at 1.8 MPa as a function of gas temperature (a 200 °C; b 250 °C; c 300 °C; d 350 °C; e 400 °C)

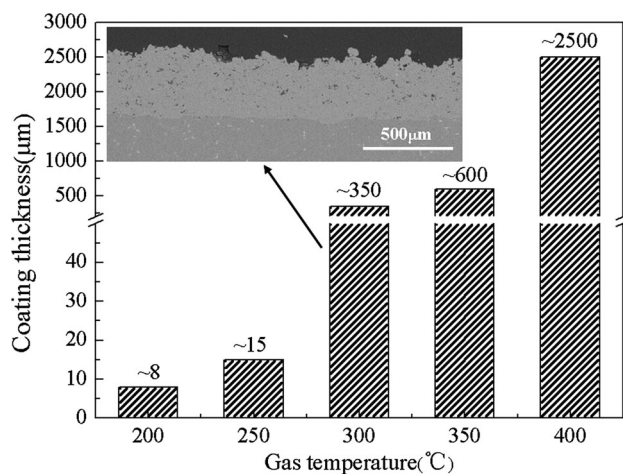


**Fig. 6** Variation in the thickness of Al-12Si coatings deposited at 1.8 MPa with gas temperature rising

temperatures are increased to 350 and 400 °C. The coating porosity increases rather than decreases with the rise of gas temperature, which indicates an excessive gas temperature has a negative effect on coating porosity. The increased porosity in the coatings deposited at 350 and 400 °C can be attributed to two phenomena. First, there may be little deformation of the large particles in the coatings due to low ductility of Al-12Si, as shown in Fig. 8(c). The other important phenomenon could be the reduced peening effect of resilient particles. As more particles reach critical velocities for deposition, there is a decrease in the number of resilient particles, which reduces the peening effect of powder particles on the coatings.

In conclusion, the optimal gas pressure and gas temperature are 1.8 MPa and 300 °C, and the spraying distance is 10 mm. The ideal Al-12Si coatings must be thicker and have low porosity and high deposition efficiency. In

this study, it is demonstrated that the combined action of gas pressure and gas temperature is critical to produce high-quality Al-12Si coatings.

### 3.4 XRD Analysis

The important work, in this section, investigates the influence of cold spray on phase composition of Al-12Si coatings. The XRD patterns of Al-12Si powders and cold-sprayed Al-12Si coatings deposited at the optimal spray parameters (1.8 MPa, 300 °C and 10 mm) are shown in

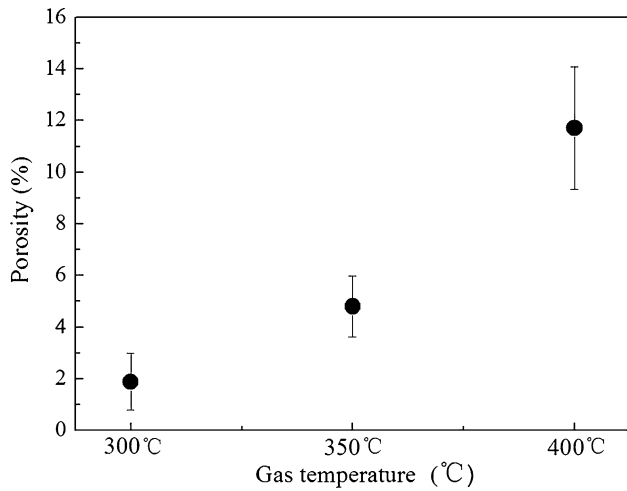


**Fig. 7** Influence of gas temperature (300, 350, 400 °C) on the porosity of Al-12Si coatings deposited at 1.8 MPa

Fig. 9. As can be seen from Fig. 9, the  $\alpha$ -Al and Si diffraction peaks of powders can be accurately identified. What is more, the positions of  $\alpha$ -Al and Si diffraction peaks of coatings are completely consistent with those of powders, and no other diffraction peaks are found in XRD pattern of coatings. The result is similar to the result of Li (Ref 33). This suggests that Al-12Si coatings are characterized by no new phase, no lattice distortion and no obvious change in oxidation because of the very low gas temperature during cold spray process. The crystal

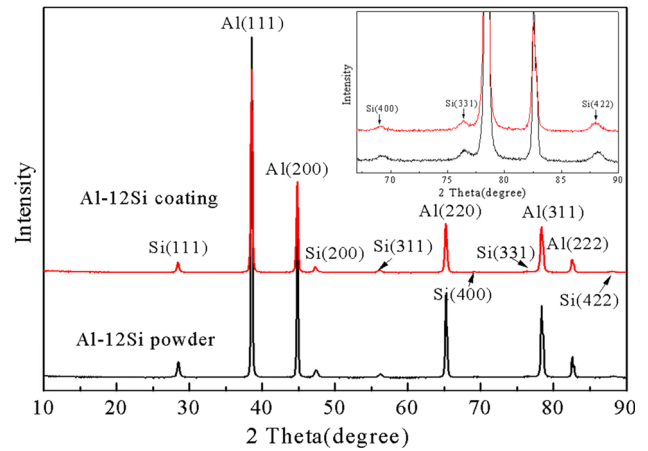


**Fig. 9** XRD patterns of Al-12Si powders and cold-sprayed Al-12Si coatings deposited at 1.8 MPa, 300 °C, and 10 mm

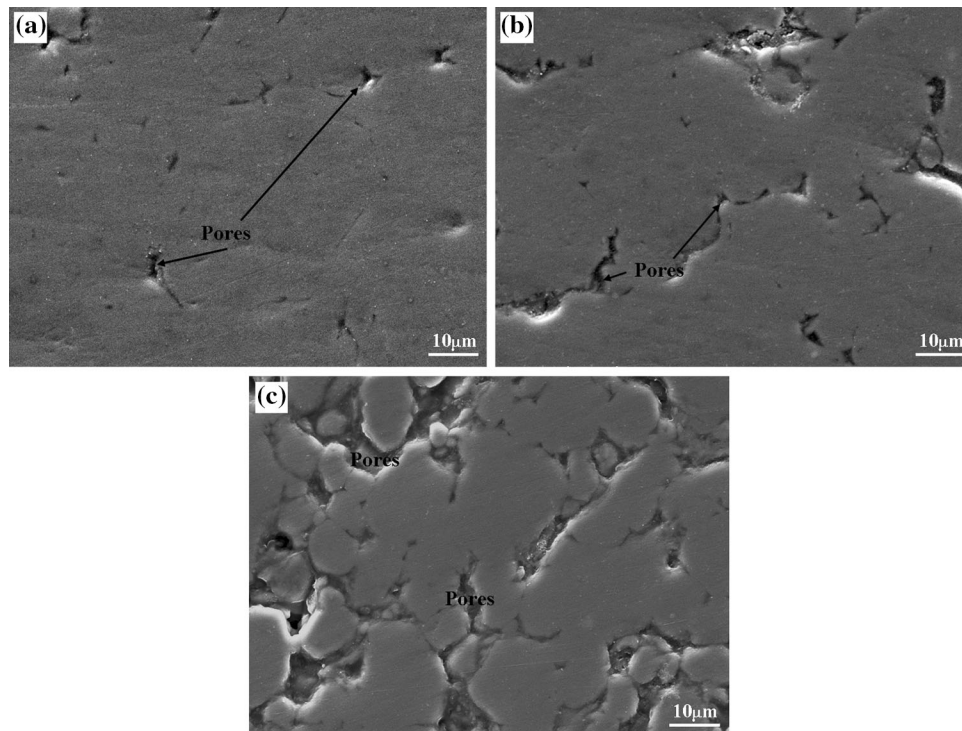


**Fig. 8** The microstructures of these coatings deposited at 1.8 MPa as a function of gas temperatures (a 300 °C; b 350 °C; c 400 °C)

structure of coatings is completely identical with that of powders.

### 3.5 Microhardness

Compared with pure Al, the existence of Si phase generates large variations in coating hardness. The Al-12Si coatings with relatively high hardness can be produced by cold spray. The microhardness measurements of AZ31 magnesium alloy, Al-12Si powders, and cold-sprayed Al-12Si coatings are shown in Fig. 10. It is found that the average microhardness value of AZ31 magnesium alloy is about  $584 \pm 49$  MPa, while those of Al-12Si powders and Al-12Si coatings are, respectively,  $995 \pm 85$  and  $994 \pm 110$  MPa. The microhardness of Al-12Si coatings in this study is slightly less than that ( $112 \pm 5\text{HV}_{300} = 1098 \pm 49$  MPa) of cold-sprayed Al-12Si coatings deposited at 773 K and 3.0 MPa in the Ref 34. It manifests that a well Al-12Si coating similarly produced at relatively low gas temperature ( $300\text{ }^\circ\text{C} = 573$  K) and gas pressure (1.8 MPa). The produced Al-12Si coatings are found to be 70% harder than AZ31 magnesium alloy. Compared with Al-12Si powders, the Al-12Si coatings have similar microhardness. The Al-12Si coatings, therefore, provide a good level of protection for AZ31 magnesium alloy under wear environment (Ref 35).

### 3.6 Adhesion Strength

The formation of a cold-sprayed coating is a result of plastic impact of powder particles at high velocity and low

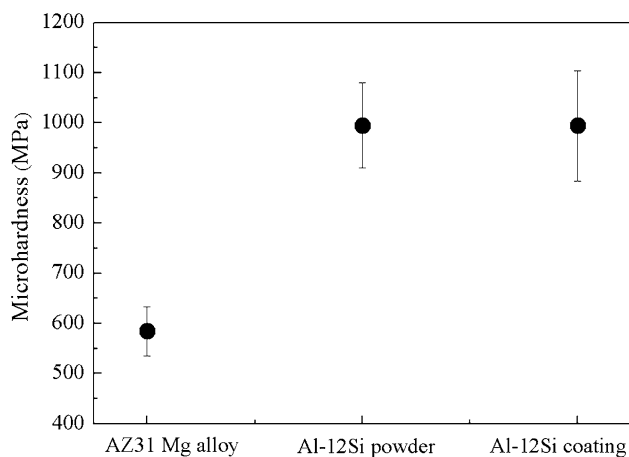


**Fig. 10** Microhardness measurements of AZ31 magnesium alloy, Al-12Si powders, and cold-sprayed Al-12Si coatings

temperature. The adhesion between particle and substrate results from large plastic deformation under high pressure and strain rate. The adhesion strength is a significant standard for evaluating coating quality. Table 4 provides the adhesion strength between the cold-sprayed Al-12Si coatings and two kinds of substrates including AZ31 magnesium alloy in this study and mild steel previously reported by Li et al. (Ref 36). The adhesion strength between Al-12Si coatings and AZ31 substrate is approximately  $45.01 \pm 0.44$  MPa, and the failure is at the interface between coatings and substrate. The adhesion strength between Al-12Si coatings and mild steel as prepared by Li et al. is not  $< 50$  MPa, and no failure occurs in the coatings due to metallurgical bonding. Compared with the process parameters (2.7 MPa,  $560\text{ }^\circ\text{C}$ ) and result in the Ref 36, the adhesion strength measured in this study is relatively high for an Al-12Si coating deposited at low pressure of 1.8 MPa and  $300\text{ }^\circ\text{C}$  (close to half of melting point).

## 4. Conclusions

The Al-12Si coatings were produced on AZ31 magnesium alloy using cold spray technology. The conclusions of this study can be summarized as follows:

1. The Al-12Si powders with particle sizes of 6 to  $40\text{ }\mu\text{m}$  possess a near-spherical shape and fine-scaled dendritic microstructure.
2. The gas pressure and gas temperature are two critical factors for obtaining high-quality coatings. The influence of gas pressure on coatings at low gas temperature is much smaller than that at high gas temperature, and the excessive gas temperature has a negative effect on coatings. The deposited Al-12Si coatings have the same crystal structure with powders, sufficient thickness, and low porosity (below 2%) under optimal process parameters of 1.8 MPa,  $300\text{ }^\circ\text{C}$ , and 10 mm.
3. The cold-sprayed Al-12Si coatings have an average microhardness of about  $994 \pm 110$  MPa which is 70% harder than AZ31 magnesium alloy.
4. The adhesion strength between Al-12Si coatings and AZ31 substrate is approximately  $45.01 \pm 0.44$  MPa, which is relatively high for Al-12Si coatings deposited at low pressure of 1.8 MPa and  $300\text{ }^\circ\text{C}$ , showing a fine bonding between coatings and substrate.

**Table 4** Adhesion strength between the cold-sprayed Al-12Si coatings and two kinds of substrates

Coating type	Substrate	Gas pressure, MPa	Gas temperature, $^\circ\text{C}$	Adhesion strength, MPa	Tensile failure position
Al-12Si	AZ31 magnesium alloy	1.8	300	$45.01 \pm 0.44$	Coating/substrate interface
Al-12Si (Ref 36)	Mild steel	2.7	560	$> 50$	In adhesive



## References

1. Y.S. Tao, T.Y. Xiong, C. Sun, H.Z. Jin, H. Du, and T.F. Li, Effect of  $\alpha$ -Al<sub>2</sub>O<sub>3</sub> on the Properties of Cold Sprayed Al/ $\alpha$ -Al<sub>2</sub>O<sub>3</sub> Composite Coatings on AZ91D Magnesium Alloy, *Appl. Surf. Sci.*, 2009, **256**(1), p 261-266
2. A. Pardo, M.C. Merino, M. Mohedano, P. Casajús, A.E. Coy, and R. Arrabal, Corrosion Behaviour of Mg/Al Alloys with Composite Coatings, *Surf. Coat. Technol.*, 2009, **203**(9), p 1252-1263
3. X.G. Sun, M. Nouri, Y. Wang, and D.Y. Li, Corrosive Wear Resistance of Mg-Al-Zn Alloys with Alloyed Yttrium, *Wear*, 2013, **302**(1-2), p 1624-1632
4. Y.S. Tao, T.Y. Xiong, C. Sun, L.Y. Kong, X.Y. Cui, T.F. Li, and G.L. Song, Microstructure and Corrosion Performance of a Cold Sprayed Aluminium Coating on AZ91D Magnesium Alloy, *Corros. Sci.*, 2010, **52**(10), p 3191-3197
5. K.K. Ajith Kumar, U.T.S. Pillai, B.C. Pai, and M. Chakraborty, Dry Sliding Wear Behaviour of Mg-Si Alloys, *Wear*, 2013, **303**(1-2), p 56-64
6. M. Campo, M. Carboneras, M.D. López, B. Torres, P. Rodrigo, E. Otero, and J. Rams, Corrosion Resistance of Thermally Sprayed Al and Al/SiC Coatings on Mg, *Surf. Coat. Technol.*, 2009, **203**(20-21), p 3224-3230
7. I. Saeki, T. Seguchi, Y. Kourakata, and Y. Hayashi, Ni Electroplating on AZ91D Mg Alloy Using Alkaline Citric Acid Bath, *Electrochim. Acta*, 2013, **114**, p 827-831
8. Z.C. Shao, Z.Q. Cai, R. Hu, and S.Q. Wei, The Study of Electroless Nickel Plating Directly on Magnesium Alloy, *Surf. Coat. Technol.*, 2014, **249**, p 42-47
9. M.A. Taha, N.A. El-Mahallawy, R.M. Hammouda, and S.I. Nassef, PVD Coating of Mg-AZ31 by Thin Layer of Al and Al-Si, *J. Coat. Technol. Res.*, 2010, **7**(6), p 793-800
10. C.C. Liu, J. Liang, J.S. Zhou, L.Q. Wang, and Q.B. Li, Effect of Laser Surface Melting on Microstructure and Corrosion Characteristics of AM60B Magnesium Alloy, *Appl. Surf. Sci.*, 2015, **343**, p 133-140
11. B. Gao, S.Z. Hao, J.X. Zou, W.Y. Wu, G.F. Tu, and C. Dong, Effect of High Current Pulsed Electron Beam Treatment on Surface Microstructure and Wear and Corrosion Resistance of an AZ91HP Magnesium Alloy, *Surf. Coat. Technol.*, 2007, **201**(14), p 6297-6303
12. X.M. Wang, X.Q. Zeng, G.S. Wu, S.S. Yao, and Y.J. Lai, Surface Analysis and Oxidation Behavior of Y-ion Implanted AZ31 Magnesium Alloys, *Appl. Surf. Sci.*, 2007, **253**(7), p 3574-3580
13. S. Durdu, A. Aytac, and M. Usta, Characterization and Corrosion Behavior of Ceramic Coating on Magnesium by Micro-Arc Oxidation, *J. Alloys Compd.*, 2011, **509**(34), p 8601-8606
14. L.F. Hu, Q.S. Meng, S.P. Chen, and H. Wang, Effect of Zn Content on the Chemical Conversion Treatments of AZ91D Magnesium Alloy, *Appl. Surf. Sci.*, 2012, **259**, p 816-823
15. S.J. Kim, Y. Zhou, R. Ichino, M. Okido, and S. Tanikawa, Characterization of the Chemical Conversion Films that Form on Mg-Al Alloy in Colloidal Silica Solution, *Met. Mater. Int.*, 2003, **9**(2), p 207-213
16. T. Suhonen, T. Varis, S. Dosta, M. Torrell, and J.M. Guilemany, Residual Stress Development in Cold Sprayed Al, Cu and Ti Coatings, *Acta Mater.*, 2003, **61**(17), p 6329-6337
17. M.R. Rokni, C.A. Widener, and V.R. Champagne, Microstructural Stability of Ultrafine Grained Cold Sprayed 6061 Aluminum Alloy, *Appl. Surf. Sci.*, 2014, **290**, p 482-489
18. J.-O. Kliemann, H. Gutzmann, F. Gärtner, H. Hübner, C. Borchers, and T. Klassen, Formation of Cold-Sprayed Ceramic Titanium Dioxide Layers on Metal Surfaces, *J. Therm. Spray Technol.*, 2011, **20**(1-2), p 292-298
19. Y. Xu and I.M. Hutchings, Cold Spray Deposition of Thermoplastic Powder, *Surf. Coat. Technol.*, 2006, **201**(4), p 3044-3050
20. S.R. Bakshi, D. Wang, T. Price, D. Zhang, A.K. Keshri, Y. Chen, D.G. McCartney, P.H. Shipway, and A. Agarwal, Microstructure and Wear Properties of Aluminum/Aluminum-Silicon Composite Coatings Prepared by Cold Spraying, *Surf. Coat. Technol.*, 2009, **204**(4), p 503-510
21. L.Y. Kong, L. Shen, B. Lu, R. Yang, X.Y. Cui, T.F. Li, and T.Y. Xiong, Preparation of TiAl<sub>3</sub>-Al Composite Coating by Cold Spray and Its High Temperature Oxidation Behavior, *J. Therm. Spray Technol.*, 2010, **19**(6), p 1206-1210
22. H.J. Kim, C.H. Lee, and S.Y. Hwang, Superhard Nano WC-12%Co Coating by Cold Spray Deposition, *Mater. Sci. Eng. A*, 2005, **391**(1-2), p 243-248
23. A. List, F. Gärtner, T. Mori, M. Schulze, H. Assadi, S. Kuroda, and T. Klassen, Cold Spraying of Amorphous Cu<sub>50</sub>Zr<sub>50</sub> Alloys, *J. Therm. Spray Technol.*, 2015, **24**(1-2), p 108-118
24. D. Poirier, J.G. Legoux, R.A.L. Drew, and R. Gauvin, Consolidation of Al<sub>2</sub>O<sub>3</sub>/Al Nanocomposite Powder by Cold Spray, *J. Therm. Spray Technol.*, 2011, **20**(1-2), p 275-284
25. K.H. Ko, J.O. Choi, and H. Lee, Intermixing and Interfacial Morphology of Cold-Sprayed Al Coatings on Steel, *Mater. Lett.*, 2014, **136**, p 45-47
26. C.C. Ma, X.F. Liu, and C.G. Zhou, Cold-Sprayed Al Coating for Corrosion Protection of Sintered NdFeB, *J. Therm. Spray Technol.*, 2014, **23**(3), p 456-462
27. V.K. Champagne, The Repair of Magnesium Rotorcraft Components by Cold Spray, *J. Fail. Anal. Prev.*, 2008, **8**(2), p 164-175
28. J. Clarke and A.D. Sarkar, Wear Characteristics of As-Cast Binary Aluminium-Silicon Alloys, *Wear*, 1979, **54**(1), p 7-16
29. T.T. Wong and G.Y. Liang, Effect of Laser Melting Treatment on the Structure and Corrosion Behaviour of Aluminium and Al-Si Alloys, *J. Mater. Process. Technol.*, 1997, **63**(1-3), p 930-934
30. K.H. Baik and P.S. Grant, Microstructural Evaluation of Monolithic and Continuous Fibre Reinforced Al-12wt.%Si Produced by Low Pressure Plasma Spraying, *Mater. Sci. Eng. A*, 1999, **265**(1-2), p 77-86
31. L. Zhao, K. Bobzin, D.Y. He, J. Zwick, F. Ernst, and E. Lugscheider, Deposition of Aluminium Alloy Al12Si by Cold Spraying, *Adv. Eng. Mater.*, 2006, **8**(4), p 264-267
32. J.W. Wu, J.G. Yang, H.Y. Fang, S. Yoon, and C. Lee, The Bond Strength of Al-Si Coating on Mild Steel by Kinetic Spraying Deposition, *Appl. Surf. Sci.*, 2006, **252**(22), p 7809-7814
33. W.-Y. Li, C. Zhang, X.P. Guo, G. Zhang, H.L. Liao, and C. Coddet, Deposition Characteristics of Al-12Si Alloy Coating Fabricated by Cold Spraying with Relatively Large Powder Particles, *Appl. Surf. Sci.*, 2007, **253**(17), p 7124-7130
34. M. Yandouzi, P. Richer, and B. Jodoin, SiC Particulate Reinforced Al-12Si Alloy Composite Coatings Produced by the Pulsed Gas Dynamic Spray Process: Microstructure and Properties, *Surf. Coat. Technol.*, 2009, **203**(20-21), p 3260-3270
35. D.H. Jeong, U. Erb, K.T. Aust, and G. Palumbo, The relationship between Hardness and Abrasive Wear Resistance of Electrodeposited Nanocrystalline Ni-P Coatings, *Scr. Mater.*, 2003, **48**(8), p 1067-1072
36. W.-Y. Li, C. Zhang, X.P. Guo, C.-J. Li, H.L. Liao, and C. Coddet, Study on Impact Fusion at Particle Interfaces and Its Effect on Coating Microstructure in Cold Spraying, *Appl. Surf. Sci.*, 2007, **254**(2), p 517-526